Available online at www.sciencedirect.com
SCIENCE DIRECT®

Catalysis Today 89 (2004) 431–438

CATALYSIS TODAY

www.elsevier.com/locate/cattod

Fischer–Tropsch synthesis over Co–SiO_2 catalysts prepared by the sol–gel method

Kiyomi Okabe*, Xiaohong Li[1], Mingdeng Wei, Hironori Arakawa

National Institute of Advanced Industrial Science and Technology, Tsukuba, Ibaraki 305-8565, Japan

Received 25 July 2003; received in revised form 5 December 2003; accepted 16 January 2004

Abstract

Fischer–Tropsch synthesis was carried out in slurry phase over uniformly dispersed Co–SiO_2 catalysts prepared by the sol–gel method. When 0.01–1 wt.% of noble metals were added to the Co–SiO_2 catalysts, a high and stable catalytic activity was obtained over 60 h of the reaction at 503 K and 1 MPa. The addition of noble metals increased the reducibility of surface Co on the catalysts, without changing the particle size of Co metal significantly. High dispersion of metallic Co species stabilized on SiO_2 was responsible for stable activity. The uniform pore size of the catalysts was enlarged by varying the preparation conditions and by adding organic compounds such as *N*,*N*-dimethylformamide and formamide. Increased pore size resulted in decrease in CO conversion and selectivity for CO_2, a byproduct, and an increase in the olefin/paraffin ratio of the products. By modifying the surface of wide pore silica with Co–SiO_2 prepared by the sol–gel method, a bimodal pore structured catalyst was prepared. The bimodal catalyst showed high catalytic performance with reducing the amount of the expensive sol–gel Co–SiO_2.

Keywords: Cobalt catalyst; Fischer–Tropsch synthesis; Pore size; Sol–gel method

1. Introduction

GTL (gas to liquid) process is one of the most promising ways to utilize natural gas at remote areas to form ultra-clean fuels at economically feasible cost [1]. Development of catalysts for Fischer–Tropsch (F–T) synthesis is the key technology of GTL process. One of the major issues in F–T reaction is wide molecular distribution of products. The extremely exothermic property of the reaction causes hot spots on the catalyst surface, bringing about thermal heterogeneity, resulting in a decrease in selectivity because of undesirable side reactions. In order to avoid formation of hot spots, effective thermal removal of the reaction and uniform surface structure of the catalysts are prerequisite. Slurry reactor is economically the most effectual for thermal removal. In the present paper, the second task, the uniform structure, was accomplished by preparing Co–SiO_2 catalysts by the sol–gel method, and the effects of the pore structure were investigated by varying the pore size.

2. Experimental

2.1. Catalyst preparation by the sol–gel method

Although the sol–gel method is known as one of the easiest ways to obtain uniform structure, the microscopic feature depends on the detailed preparation method employed [2–4]. When the procedure is inadequate, Co–O–Si bond is atomically non-uniform, and the structure of obtained Co–SiO_2 gel is almost the same as Co/SiO_2 prepared by impregnation, even if the gel seems apparently homogeneous. The sol–gel procedure employed in this study is as described previously in detail [5–7]. The required amount of $Co(NO_3)_2 \cdot 6H_2O$ was dissolved in ethylene glycol. Tetraethyl orthosilicate (TEOS) was added to the solution, and the mixture was heated with vigorous stirring to form a homogeneous solution. A pore size modifier consisted of various organic compounds, such as *N*,*N*-dimethylformamide (DMF),

---

* Corresponding author. Fax: +81-29-861-4487.
E-mail address: kiyo-okabe@aist.go.jp (K. Okabe).

[1] Present address: The University of Kitakyushu, Hibikino, Kitakyushu, Fukuoka 808-0135, Japan.

0920-5861/$ – see front matter © 2004 Elsevier B.V. All rights reserved.
doi:10.1016/j.cattod.2004.01.005

formamide (FA), and polyethylene glycol (PEG; average molecular weight = 2000), and a precursor of promoter (MCl_x) were added to the solution at this stage. Distilled water diluted with ethanol was then added to the solution dropwise at room temperature, resulting in a homogeneous clear sol. The sol was slowly hydrolyzed by heating at a temperature higher than 353 K for more than 40 h, to form a glassy transparent gel. The gel was dried and calcined in N_2 and air flows at 823 K for 15 h, and then reduced in a H_2 flow at 773 K for 15 h to form 20 wt.% Co–M–SiO_2(SG) catalyst (M: promoter).

A bimodal catalyst was prepared by modifying the surface of wide pore silica (Fuji Silisia, Q-30; average pore diameter = 30 nm) with the Co–M–SiO_2(SG), according to the similar method reported by Tsubaki et al. [8]. The finely ground Q-30 silica was suspended into the clear sol of Co–M–SiO_2 described above, and the mixture was gelled at 353 K with vigorous stirring. The gel was similarly dried, calcined, and then reduced to form 20 wt.% Co–M–SiO_2(SG)/Q-30.

2.2. Fischer–Tropsch synthesis

After passivation, 2.0 g of the reduced catalyst was ground into fine powder, and suspended in 50 cm^3 of hexadecane under an inert atmosphere. The catalyst slurry was packed into an autoclave-type reactor of about 100 cm^3, and synthesis gas containing 10% Ar was bubbled into the slurry with vigorous stirring in the flow system. The dissolution of the gas into the slurry was promoted by a specially designed stirring tubular T-rod with small holes at the upper part. When the stirring rate was higher than 600 rpm, the reaction gas over the slurry was aspirated into the rod through the holes, and bubbled out from the ends of the tubular T-rod, probably owing to centrifugal force. Thus, the gas-phase syngas was effectively circulated in the reactor through the stirring rod, and the complete mixing system was accomplished [9,10].

The reaction conditions were as follows: $H_2/CO = 2/1$, $T = 503\,K$, $P = 1\,MPa$, and $W/F = 10$ g-catal. h/mol. The effluent gas was periodically analyzed by on-line gas chromatography, and the contents of inorganic gases and $C_{1–14}$ hydrocarbons were determined, with using Ar in the sample gas as the internal standard. The contents of C_{11+} hydrocarbons in the slurry were determined separately by gas chromatography after the reaction.

2.3. Characterization of catalysts

Multi point BET surface area, pore volume, and BJH pore size distribution of the catalysts were calculated from the adsorption–desorption isotherm of N_2 at 77 K, using an automatic gas adsorption apparatus, ASAP-2000. The metallic surface area of the catalyst was determined by H_2 adsorption at 308 K, using ASAP-2000. X-ray photoelectron spectra of the catalysts were recorded with Shimadzu ESCA-850 without exposure to open-air after pretreatment at 773 K in a flow of H_2 within the pre-chamber of the apparatus. The binding energies of XPS were referred to evaporated Au on the surface of the sample as the internal standard with Au $4f_{7/2}$ level at 83.8 eV. The reduction of the catalysts was evaluated by temperature-programmed reduction (TPR) heating up to 1200 K at a rate of 10 K/min in a flow of H_2 at a rate of 50 cm^3/min, using Shimadzu TGA-51. Transmission electron microscopy (TEM) images were obtained on a Jeol JEM-2000FX operated at 200 kV. The TEM sample was deposited as a dry powder on a thin carbon film mounted on a copper grid. X-ray powder diffraction (XRD) patterns were recorded using a Mac Science MPX-18 diffractometer with Cu Kα irradiation (40 kV, 150 mA).

3. Results and discussion

3.1. Structure of catalysts prepared by the sol–gel method

The pore size distribution curves derived from N_2 desorption from catalysts are shown in Fig. 1.((a) and (b): Co/SiO_2(SG) catalysts prepared by the sol–gel method, and (c): Co/SiO_2(Imp) catalyst prepared by impregnation, respectively.) The catalyst (c) supported on a commercial silica (Q-10) showed wide distribution of pore size. In contrast, the distribution curves of the sol–gel catalysts ((a) and (b)) were very sharp with a peak maximum at about 4 nm irrespective of the Co content, indicating that the pore structure of Co–SiO_2(SG) was more uniform than that of Co/SiO_2(Imp).

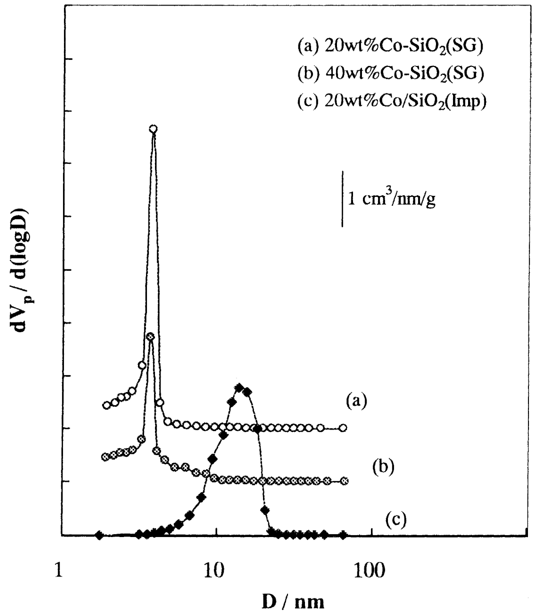

Fig. 1. Pore size distribution of (a) 20 wt.% Co–SiO_2(SG) prepared by the sol–gel method, (b) 40 wt.% Co–SiO_2(SG) prepared by the sol–gel method, and (c) 20 wt.% Co/SiO_2(Imp) prepared by impregnation. (Reprinted with permission from [6], Copyright (1999) The Japan Petroleum Institute.)

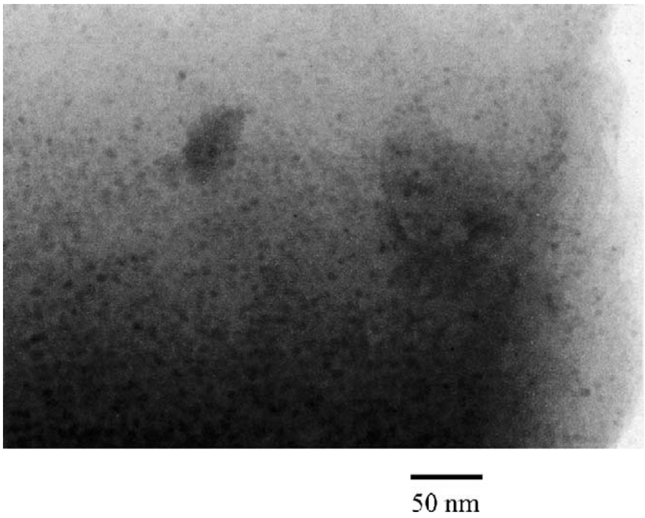

Fig. 2. TEM image of 40 wt.% Co–SiO_2(SG) catalyst prepared by the sol–gel method.

The TEM observation displayed that Co metal particles with a diameter of 3–5 nm were uniformly dispersed in the Co–SiO_2(SG) catalysts, as shown in Fig. 2. The XPS depth profile analysis of the Co–SiO_2(SG) catalysts indicated that the Co concentration was three-dimensionally uniform, too.

XRD patterns of the Co/SiO_2(Imp) catalysts clearly showed peaks corresponding to Co metal. From the line broadening of the peaks, the crystallite size was estimated at 26–28 nm for the fresh and used catalysts, respectively. In contrast, the peaks were not obvious for the Co–Ir–SiO_2(SG) catalysts, and the crystallite size was difficult to estimate by XRD line broadening, implying high dispersion of Co, even in highly loaded Co–SiO_2(SG) catalysts up to 60 wt.% Co. Such a highly loaded catalyst was difficult to prepare by impregnation, because of the restriction of the pore volume (V_p); i.e. such a large amount of $Co(NO_3)_2$ is difficult to dissolve in water of the same volume as V_p by the incipient wetness technique of impregnation. The sol–gel method proved to be more suitable for the uniform preparation of highly loaded catalysts than the impregnation method.

3.2. Fischer–Tropsch reaction over catalysts prepared by the sol–gel method

Fig. 3 shows time course of F–T reaction in slurry phase over (a) 20 wt.% Co/SiO_2(Imp), (b) 20 wt.% Co–0.1 wt.% Ir–SiO_2(SG), (c) 20 wt.% Co–SiO_2(SG), and (d) 0.1 wt.% Ir/SiO_2(SG) catalysts. The conventional Co/SiO_2(Imp) catalyst was rapidly deactivated during the reaction, though it showed high initial activity. In contrast, CO conversion of the Co–SiO_2(SG) catalysts without promoter (Fig. 3(c)) was much lower than that of the Co/SiO_2(Imp) catalyst. The small amount of chemisorbed H_2 on the Co–SiO_2(SG) catalyst corresponded to its low activity. However, when a trace amount of noble metal was added to the Co–SiO_2(SG) catalyst, the catalytic activity drastically increased, and no deactivation was observed as shown in Fig. 3(b). It is suggested that the uniform structure of the sol–gel catalysts was responsible for the stable activity. The fact that Ir/SiO_2(SG) catalyst (d) did not show any F–T reaction activity implies synergistic effect between the small amount of Ir and the Co/SiO_2(SG) catalyst on high activity. The similar synergism has been also reported on Co–Pd/SiO_2 catalysts, of which Co/Pd ratio is in the range of 2/1–1/2 [11]. In contrast, such a synergistic effect was not clear on our Co/SiO_2(Imp) catalyst prepared by impregnation, since the catalytic activity hardly increased by adding Ir to Co/SiO_2(Imp).

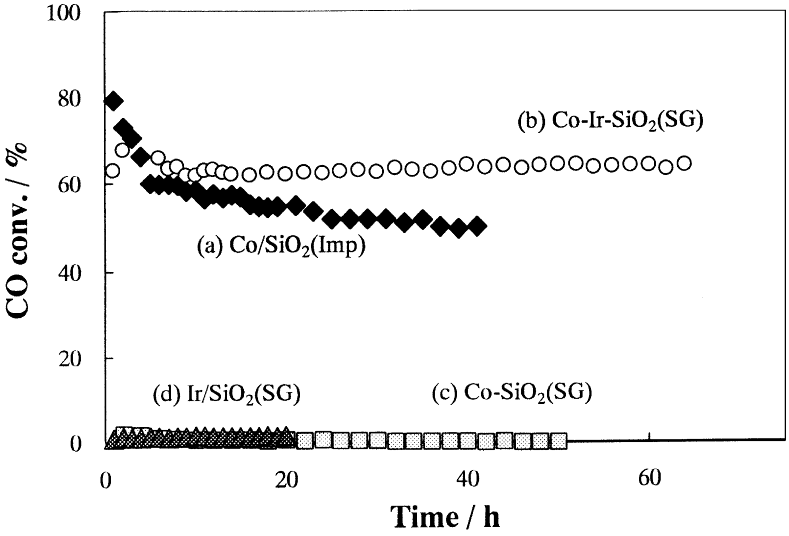

Fig. 3. Time course of F–T reaction in slurry phase over (a) 20 wt.% Co/SiO_2(Imp), (b) 20 wt.% Co–0.1 wt.% Ir–SiO_2(SG), (c) 20 wt.% Co–SiO_2(SG), and (d) 0.1 wt.% Ir/SiO_2(SG) catalysts, at $T = 503$ K, $P = 1$ MPa, $H_2/CO = 2/1$, and $W/F = 10$ g-catal. h/mol. (Reprinted with permission from [6], Copyright (1999) The Japan Petroleum Institute.)

Table 1
Effect of noble metal promoters on F–T reaction over Co–SiO_2 catalysts prepared by the sol–gel method[a]

Promoter (M)	CO conversion (%)	Selectivity (%)			
		CH_4	CO_2	C_{5+}	α[b]
–	0.0	–	–	–	–
Re	51.3	19.5	1.8	59.6	0.81
Ru	53.8	11.8	2.8	62.9	0.80
Rh	59.5	18.1	6.7	50.2	0.76
Ir	60.6	13.3	2.7	68.3	0.84
Pd	44.0	15.3	1.5	61.2	0.78

[a] Catalyst: 20 wt.% Co–0.1 wt.% M–SiO_2(SG), where M is noble metal.

[b] Chain growth probability of CH_x intermediate determined by Anderson–Schultz–Flory plot of hydrocarbon products.

The effect of various noble metal promoters on F–T reaction is summarized in Table 1. Since almost no deactivation was observed, the average values throughout the reaction were tabulated. Every promoter (M) listed increased the activity of 20 wt.% Co–SiO_2(SG) catalyst, by loading 0.1 wt.% of M. Among the promoters, Ir showed the highest CO conversion and C_{5+} selectivity, with restraining CH_4 formation. The effect of loading amount of Ir was investigated and illustrated in Fig. 4. Even an addition of 0.01 wt.%–Ir was sufficient for the promotion. It suggests that spilt-over hydrogen on Ir is responsible for the activation of Co on the surface [12].

3.3. Characterization of Co–SiO_2(SG) catalyst promoted by noble metal

In order to elucidate the promoting effects by the noble metals, the catalysts were characterized by XPS, TPR, and chemisorption. Fig. 5 shows TPR spectra of (a) 40 wt.% Co–SiO_2(SG), (b) 40 wt.% Co–1 wt.% Ir–SiO_2(SG), and (c) 20 wt.% Co/SiO_2(Imp) catalysts. The most of Co in the sol–gel catalyst without promoter was difficult to reduce below 1000 K, suggesting strong Co–O–Si bond to form Co-silicate like structure. XRD measurement confirmed the formation of Co_2SiO_4 by calcining Co–SiO_2(SG) at a high temperature above 900 K. In contrast, the sol–gel catalyst promoted with Ir was readily reduced as Co/SiO_2(Imp) prepared by impregnation, which was reduced at a low temperature about 600 K. The adsorbed amount of H_2 and the % reduction of surface Co (%-Co^0) on the catalysts after pretreatment with H_2 at 773 K are summarized in Table 2. The %-Co^0 determined by XPS should be, however, regarded as qualitative reduction degree, since XPS provides information of external surface of the sample only. It clearly indicates that Ir is responsible for the reduction of the surface Co in Co–SiO_2(SG) prepared by the sol–gel method.

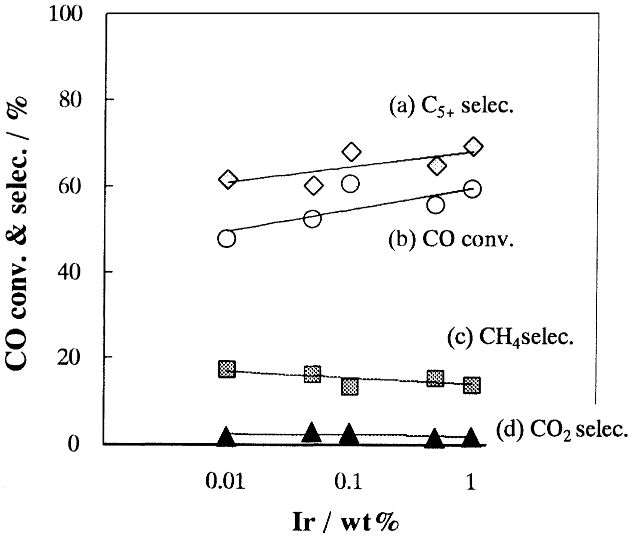

Fig. 4. Effects of the amount of Ir promoter on F–T synthesis over 20 wt.% Co–Ir–SiO_2(SG) catalysts, at $T = 503$ K, $P = 1$ MPa, H_2/CO = 2/1, and $W/F = 10$ g-catal. h/mol. (a) C_{5+} selectivity, (b) CO conversion, (c) CH_4 selectivity, and (d) CO_2 selectivity. (Reprinted with permission from [6], Copyright (1999) The Japan Petroleum Institute.)

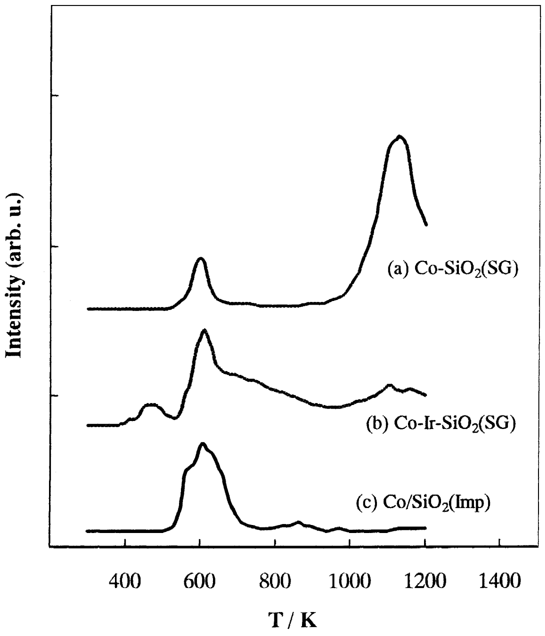

Fig. 5. TPR spectra of (a) 40 wt.% Co–SiO_2(SG), (b) 40 wt.% Co–1 wt.% Ir–SiO_2(SG), and (c) 20 wt.% Co/SiO_2(Imp) catalysts, at a heating rate of 10 K/min in H_2 flow of 50 cm^3/min. (Reprinted with permission from [6], Copyright (1999) The Japan Petroleum Institute.)

Table 2
Adsorbed amount of H_2 and %-Co^0 on catalysts, and TOF[a] (Reprinted with permission from [6], Copyright (1999) The Japan Petroleum Institute)

Catalyst	%-Co^0 determined by XPS	H_2 adsorbed ($cm^3\ g^{-1}$)	TOF (s^{-1})
20 wt.% Co/SiO_2(Imp)	52	0.42	0.11
40 wt.% Co–SiO_2(SG)	<5	<0.01	–
40 wt.% Co–1 wt.% Ir–SiO_2(SG)	35	0.16	0.34

[a] Turn-over frequency.

The promotion of Co reducibility by noble metals has been also investigated on Ru−Co/Al_2O_3 catalysts [13,14], Re−Co/Al_2O_3 catalysts [15], and so on [16]. The number of active sites evaluated by the H_2 amount adsorbed was, however, still smaller on Co–Ir–SiO_2(SG) catalyst than on Co/SiO_2(Imp) catalyst. Consequently, turn-over frequency (TOF) of the F–T reaction was three times higher over Co–Ir–SiO_2(SG) catalyst than over Co/SiO_2(Imp) catalyst, since both catalysts showed the similar CO conversion at the steady state of the reaction, as shown in Fig. 3.

3.4. Pore size effect of Co–SiO_2 catalysts prepared by the sol–gel method

Although the noble metal promoted Co–SiO_2(SG) catalysts showed higher and more stable activity owing to the uniform structure than Co/SiO_2(Imp) catalysts, the selectivity for CH_4 was relatively higher over the former catalysts than the latter. The former catalysts showed a sharp distribution of pore size at about 4 nm, whereas the latter showed wide distribution at about 10 nm. Thus, in order to clarify the pore size effect on the reaction, the pore size of the sol–gel catalyst was changed by varying the preparation conditions.

Fig. 6 shows additive effect of the sol–gel preparation on the pore size distribution of the catalysts. The amount of the pore size modifier (organic additive) was 1 g/g-catal., and the gelation temperature (T_G) was 353 K. Addition of polyethylene glycol to the homogeneous sol at the catalyst preparation stage by the sol–gel method resulted in the pore distribution curves of the final catalysts, (b) in Fig. 6, being almost identical to the curve of the catalyst without additives (a). Although it is reported that the structure of SiO_2 is controlled via addition of PEG [17], it was difficult to change the pore size by our sol–gel method, probably because of the differences in the precise preparation conditions. In contrast, addition of *N*,*N*-dimethylformamide to the homogeneous sol caused a peak maximum at about 5 nm in the pore distribution curve of the catalyst, as shown in Fig. 6(c). The pore size increased with the amount of the additive up to 2 g/g-catal., and then leveled off. Addition of formamide caused the pore distribution curve to a peak at about 6 nm (d), and the width became wider than (c). The addition of FA gave rise to a decrease of uniformity of the pore structure, along with enlargement of the pore size of the catalyst.

Fig. 7 shows the effect of gelation temperature (T_G) on pore size of the Co–Ir–SiO_2(SG) catalysts with FA addition (2 g/g-catal.). Pore size increased linearly with T_G. At a higher temperature, gelation occurred almost instantaneously. From this result, the reaction rate of gelation may sensitively affect the pore size of the final gel.

The chemical state of Co on the reduced catalysts was investigated by H_2 chemisorption to evaluate the number of active sites on the surface. The adsorption amount was in the range of 0.11–0.16 cm^3/g over the catalysts prepared above, and no drastic variation was observed.

Fig. 8 illustrates the F–T reaction results using the 20 wt.% Co–0.1 wt.% Ir–SiO_2(SG) catalysts with various pore sizes. CO conversion (a) and selectivity for CO_2 (d) decreased, and the olefin/paraffin ratio (o/p) of $C_{2–4}$ hydrocarbon products (b) increased with the mean pore diameter of the catalysts. However, CH_4 selectivity (c), as well as the α-value, was not varied significantly with the pore size. It is reported that wide pore catalysts are preferable for higher conversion and higher C_{5+} selectivity, because of higher reducibility of large

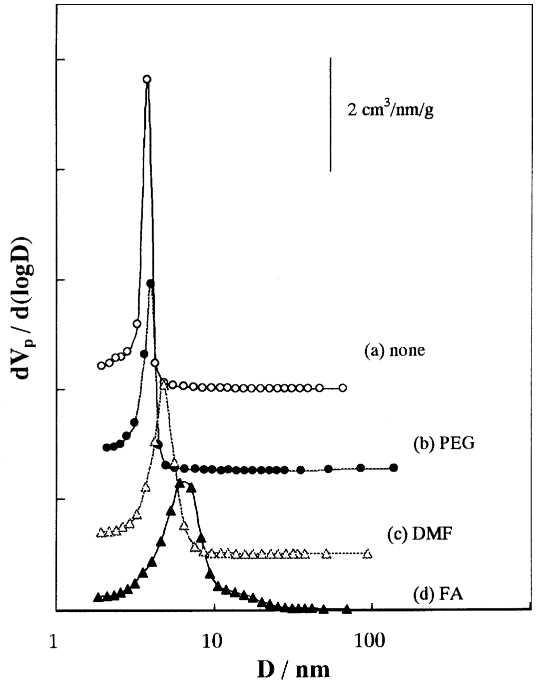

Fig. 6. Pore size distribution of 20 wt.% Co–0.1 wt.% Ir–SiO_2(SG) catalysts prepared by the sol–gel method (a) without additive, and with addition of (b) polyethylene glycol, (c) *N*,*N*-dimethylformamide and (d) formamide. Additive amount = 1 g/g-catal. (Reprinted with permission from [7], Copyright (2001) The Japan Petroleum Institute.)

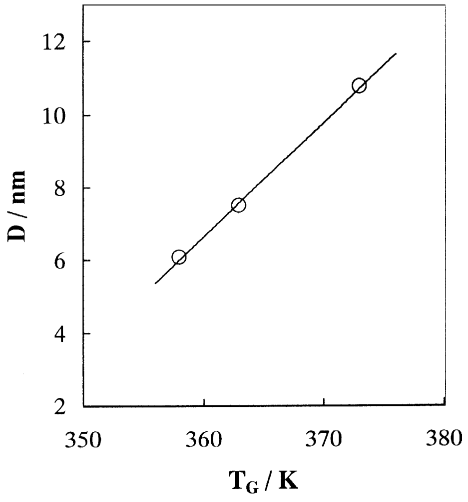

Fig. 7. Effect of gelation temperature (T_G) on pore diameter of 20 wt.% Co–0.1 wt.% Ir–SiO_2(SG) catalysts prepared by the sol–gel method.

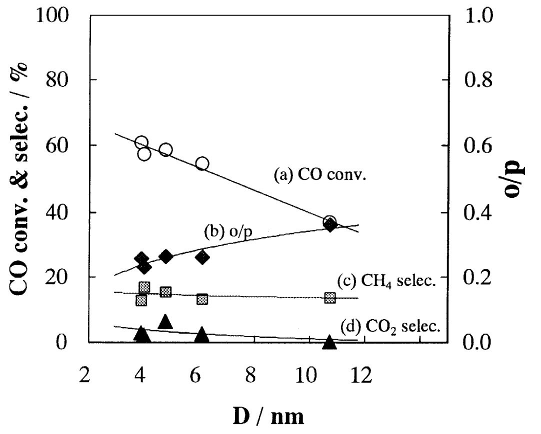

Fig. 8. Effect of pore diameter of 20 wt.% Co–0.1 wt.% Ir–SiO$_2$(SG) catalysts on F–T reaction at $T = 503$ K, $P = 1$ MPa, H$_2$/CO = 2/1, and $W/F = 10$ g-catal. h/mol. (a) CO conversion, (b) olefin/paraffin ratio (o/p) of C$_{2-4}$ hydrocarbon products, (c) CH$_4$ selectivity, and (d) CO$_2$ selectivity. (Reprinted with permission from [7], Copyright (2001) The Japan Petroleum Institute.)

Co particles in wide pores [18]. On the other hand, Iglesia et al. reported that C$_{5+}$ selectivity does not increase with Co particle size [19]. Over our Co–Ir–SiO$_2$(SG) catalysts, the catalytic activity did not increase with the pore diameter, since Co was sufficiently activated by Ir promoter. Actually, Co particle size of Co–Ir–SiO$_2$(SG) catalysts was slightly varied by changing the pore size, since Co was uniformly dispersed. Therefore, the pore size effect can be purely evaluated over our Co–Ir–SiO$_2$(SG) catalysts, with counting out the effects of Co particle size.

It is generally accepted that the activities of hydrogenation and water-gas-shift reaction (WGSR) increase at higher temperature, resulting in a higher yield of CO$_2$ and a lower o/p ratio of the products [20]. The characteristics of the reaction results over Co–Ir–SiO$_2$(SG) catalysts with small mean pore diameter resemble the F–T reaction results at higher temperature.

The dependency of the F–T reaction selectivity on the pore size of the catalysts is often explained in terms of the mass transfer limitation of the products, when the mean pore diameter is effectively small. Heavier wax produced in the small pores of the catalyst is considered to be hydro-cracked into lighter hydrocarbons or CH$_4$, during transport from the pore to the external surface of the catalyst, resulting in the lower α-value and lower o/p ratio [21–26].

However, the reaction results described above do not follow this expectation, but can be simply explained assuming a temperature difference between the micro-pore and the slurry. Since the F–T reaction is highly exothermic, the catalytic active sites in the pore may be at a higher temperature, when the heat transfer in the micro-pore is limited, resulting in the microscopic temperature gradient inside the particles. Therefore, more complex evaluation of the dependency of the reaction is required for the pore structure of the catalyst prepared by the sol–gel method.

3.5. Fischer–Tropsch reaction over bimodal catalyst

The promoted sol–gel catalysts with uniform structure showed high and stable F–T reaction activity as described above, and large pores were necessary for effective thermal removal from active sites in the pores. On the other hand, the catalytically effective sites are limited to the vicinity of the outer surface of catalyst particles, and practically the core of the particles hardly participates in the F–T reaction, because of diffusion limitation of high molecular weight products and/or slurry solvent [9]. When Co in the sol–gel catalyst was reduced to Co^0, some of Co^0 came out to the surface of the catalyst particles by Co–O bond cleavage, and others remained in the particles. The latter would not participate in the F–T reaction effectively. Thus, in order to design an efficient catalyst, the surface of wide pore silica was modified with mesoporous sol–gel catalyst, and catalysts with bimodal pore structure were prepared. By coating the surface of macropores of silica with mesoporous sol–gel catalyst, it is expected that the macropore diameter will be reduced to the extent of the thickness of coating, while that the mesopore diameter of sol–gel catalyst will not be greatly changed by coating. Fig. 9 shows pore size distribution of (a) the Co–Ir–SiO$_2$(SG) catalyst, (b) wide pore Q-30 silica, and (c) the bimodal catalyst, 20 wt.% Co–0.1 wt.% Ir–SiO$_2$(SG)/Q-30, with the ratio of SiO$_2$(SG):Q-30 = 1:1 by weight, respectively. The peak position corresponding to mesopores of the bimodal catalyst was almost the same as that of Co–Ir–SiO$_2$(SG), while the peak position corresponding to macropores of the bimodal catalyst shifted to smaller size side than that of Q-30 silica. Therefore, bimodal catalyst was prepared as expected.

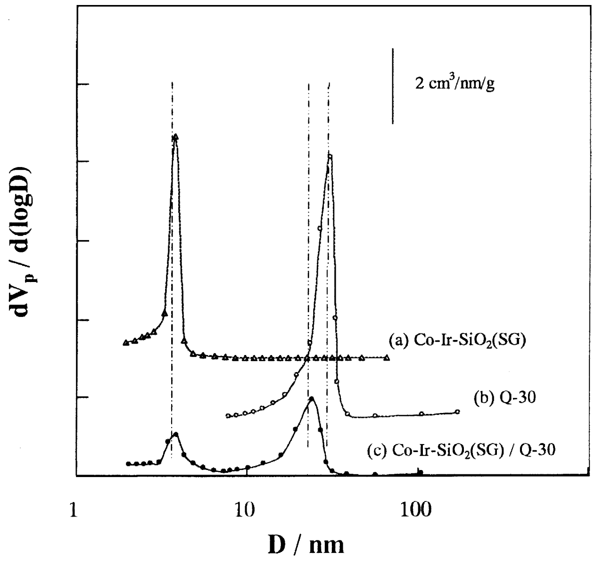

Fig. 9. Pore size distribution of (a) 20 wt.% Co–0.1 wt.% Ir–SiO$_2$(SG), (b) silica Q-30, and (c) bimodal catalyst (20 wt.% Co–0.1 wt.% Ir–SiO$_2$(SG)/Q-30) with SiO$_2$(SG):Q-30 = 1:1.

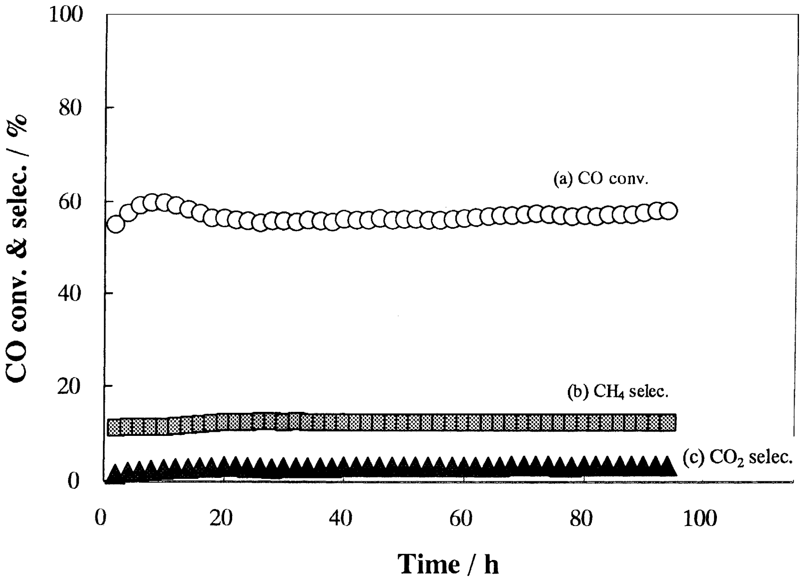

Fig. 10. Time course of F–T reaction over bimodal 20 wt.% Co–0.1 wt.% Ir–SiO_2(SG)/Q-30 catalyst, at $T = 503$ K, $P = 1$ MPa, $H_2/CO = 2/1$, and $W/F = 10$ g-catal. h/mol. (a) CO conversion, (b) CH_4 selectivity, and (c) CO_2 selectivity.

Fig. 10 illustrates the time course of F–T reaction over the bimodal catalyst. A stable activity was obtained over 90 h of the reaction, similar as 20 wt.% Co–0.1 wt.% Ir–SiO_2(SG) catalyst. The α-value of the products was 0.82. The CO conversion level was almost the same as that over Co–Ir–SiO_2(SG) catalyst, though the amount of sol–gel catalyst used was actually half. Thus, by modifying the surface of commercial wide pore silica with the sol–gel catalyst, almost the same catalytic performance was obtained with reducing the used amount of the expensive sol–gel catalyst.

From the practical point of view, durability of catalyst is crucially important. The longer term test of the reaction is now in progress to verify the stability, and the result will be reported in the near future.

4. Conclusions

Structurally uniform Co-based catalysts were prepared by the sol–gel method. While CO conversion was low over the sol–gel catalyst without promoter, addition of a trace amount of noble metal to the catalysts drastically improved the activity. The noble metal played a role in reducing surface Co of the catalyst to metallic state at low temperature. By varying the preparation conditions of the sol–gel method, the pore size was enlarged. CO conversion and CO_2 selectivity decreased, and the o/p ratio of the products increased with the pore size. By modifying the surface of wide pore silica with the sol–gel catalyst, a bimodal catalyst was prepared. The bimodal catalyst showed a high and stable activity, with reducing the used amount of the sol–gel catalyst.

Acknowledgements

This investigation was financially supported by New Energy and Industrial Technology Development Organization (NEDO) under the Project “Development of High Integration System for the Synthesis of Liquid Fuels from Natural Gas” (Contract No. 97E-10-005), and by Research for the Future Program of Japan Society for the Promotion of Science (JSPS) under the Project “Synthesis of Ecological High Quality Transportation Fuels” (Contract No. RFTF-98P01001).

References

[1] J.P. Lange, P.J.A. Tijm, Chem. Eng. Sci. 51 (1996) 2379–2387.
[2] M. Yamane, S. Inoue, A. Yasumori, J. Non-Cryst. Solids 63 (1984) 13–21.
[3] A. Yasumori, H. Kawazoe, M. Yamane, J. Non-Cryst. Solids 100 (1988) 215–219.
[4] M.A. Cauqui, J.M. Rodriguez-Izquierdo, J. Non-Cryst. Solids 147–148 (1992) 724–738.
[5] K. Okabe, K. Sayama, M. Matsubayashi, K. Shimomura, H. Arakawa, Bull. Chem. Soc. Jpn. 65 (1992) 2520–2525.
[6] K. Okabe, X. Li, T. Matsuzaki, M. Toba, H. Arakawa, K. Fujimoto, Sekiyu Gakkaishi 42 (1999) 377–382.
[7] K. Okabe, X. Li, T. Matsuzaki, H. Arakawa, K. Fujimoto, Sekiyu Gakkaishi 44 (2001) 135–139.
[8] N. Tsubaki, Y. Zhang, S. Sun, H. Mori, Y. Yoneyama, X. Li, K. Fujimoto, Catal. Comm. 2 (2001) 311–315.
[9] L. Fan, Y. Han, K. Yokota, K. Fujimoto, Sekiyu Gakkaishi 39 (1996) 111–119.
[10] K. Okabe, M. Wei, H. Arakawa, Energy & Fuels 17 (2003) 822–828.
[11] L. Guczi, Z. Schay, G. Stefler, F. Mizukami, J. Mol. Catal. A 141 (1999) 177–185.

[12] Y. Sugi, T. Matsuzaki, H. Arakawa, K. Takeuchi, T. Hanaoka, Stud. Surf. Sci. Catal. 77 (1993) 381–384.

[13] A. Kogelbauer, J.G. Goodwin Jr., R. Oukaci, J. Catal. 160 (1996) 125–133.

[14] A.R. Belambe, R. Oukaci, J.G. Goodwin Jr., J. Catal. 166 (1997) 8–15.

[15] L. Guczi, G. Stefler, Z. Koppany, L. Borko, React. Kinet. Catal. Lett. 74 (2001) 259–269.

[16] T. Matsuzaki, K. Takeuchi, T. Hanaoka, H. Arakawa, Y. Sugi, Appl. Catal. A 105 (1996) 159–184.

[17] J. Sun, W. Fan, D. Wu, Y. Sun, Stud. Surf. Sci. Catal. 118 (1998) 617–624.

[18] A.Y. Khodakov, A. Griboval-Constant, R. Bechara, V.L. Zholobenko, J. Catal. 206 (2002) 230–241.

[19] E. Iglesia, S.C. Reyes, R.J. Madon, S.L. Soled, Adv. Catal. 39 (1993) 221–302.

[20] M.E. Dry, Catal. Sci. Tech. 1 (1981) 160–255.

[21] D. Vanhove, Z. Zhang, L. Makambo, M. Blanchard, Appl. Catal. 9 (1984) 327–342.

[22] J.A. Lapszewicz, H.J. Loeh, J.R. Chipperkield, Prep. Symp. 38 (1993) 819–821.

[23] L. Fan, K. Yokota, K. Fujimoto, AIChE J. 38 (1992) 1639–1648.

[24] L. Fan, K. Yoshii, S. Yan, J. Zhou, K. Fujimoto, Catal. Today 36 (1997) 295–304.

[25] L. Fan, S. Yan, K. Fujimoto, K. Yoshii, J. Chem. Eng. Jpn. 30 (1997) 557–562.

[26] S. Yan, L. Fan, Z. Zhang, J. Zhou, K. Fujimoto, Appl. Catal. A 171 (1998) 247–254.